Journal of The Electrochemical Society

The Electrochemical Society
Advancing solid state & electrochemical science & technology

OPEN ACCESS

Steps Towards the Use of TiS_2 Electrodes in Ca Batteries

To cite this article: R. Verrelli *et al* 2020 *J. Electrochem. Soc.* **167** 070532

Journal of The Electrochemical Society, 2020 **167** 070532

Steps Towards the Use of TiS_2 Electrodes in Ca Batteries

R. Verrelli,[1,2] A. Black,[1,2] R. Dugas,[1,2] D. Tchitchekova,[1,2] A. Ponrouch,[1,2,*] and M. R. Palacin[1,2,*,z]

[1]*Institut de Ciència de Materials de Barcelona (ICMAB-CSIC) Campus UAB, E-08193 Bellaterra, Catalonia, Spain*
[2]*ALISTORE ERI European Research Institute*

A comparative study of the reduction of TiS_2 in diverse electrolyte formulations involving $Ca(BF_4)_2$ and $Ca(TFSI)_2$ salts was carried out at different temperatures (from 25 °C to 100 °C). While for the former salt intercalation of calcium is only observed at high temperatures, calcium intercalated phases are also observed for the latter even at room temperature. The nature of the electrolyte does also have an impact on the relative amounts of the phases formed. Since $Ca(TFSI)_2$ based electrolytes do not enable calcium plating, cycling was attempted using activated carbon as counterelectrode, and the reversibility of the process was ascertained. Even if corrosion of stainless steel current collectors and side reactions do still prevent proper cyclability, the results achieved should contribute to the establishment of reliable and viable cell set-up and methodology for the unambiguous study of the intercalation process in multivalent battery systems.

 [DOI: 10.1149/1945-7111/ab7a82]

Manuscript submitted December 31, 2019; revised manuscript received February 5, 2020. Published March 6, 2020. *This paper is part of the JES Focus Issue on Challenges in Novel Electrolytes, Organic Materials, and Innovative Chemistries for Batteries in Honor of Michel Armand.*

As battery technologies are widening their field of applications, embracing new technologies is certainly a path to follow. Exploration of multivalent battery chemistries is both motivated by scientific curiosity and appealing potential figures-of-merit for performance, especially in terms of energy density.[1] Thus, the use of metal anodes and multivalent cations as charge carriers has recently re-emerged as a field to explore.[2–4] Even if slow kinetics related to diffusion of multivalent ions are expected to somewhat penalize power performance, the use of covalent cathodes (such as sulfides) has proved successful.[5,6] Amongst multivalent metals calcium has recently attracted the interest of the scientific community, and diverse electrolyte formulations enabling reversible plating and stripping have been unraveled.[7–10] Yet, assessing the viability of potential cathode materials is complex. Indeed, the know how gained in the development of the Li-ion technology cannot be directly transferred due to the lack of standards, and potential side reactions. A rigorous methodology is hence a must if reliable results are to be achieved.[11,12]

In this paper we present experimental efforts towards achieving proof of concept for a Ca based technology. TiS_2 was chosen as positive electrode material for several reasons: (i) feasibility of electrochemical intercalation of calcium ions being recently assessed, despite at 100 °C and solvent co-intercalation[13] and (ii) available knowledge on intercalation chemistry derived from the studies carried out in the 70's,[14] which also include lithium based prototypes operating at high temperature using polymer electrolytes developed by M. Armand and coworkers.[15] The crystal structure of TiS_2 consists of two hexagonally close-packed sulfide layers between which reside the titanium atoms in octahedral sites. These building units are stacked together leaving a van der Waals gap in which intercalation of a range of neutral or charged species is possible, the latter concomitant to reduction of titanium. The first attempts to intercalate alkaline earth ions in TiS_2 were carried out in the 70's independently by Schöllhorn et al.[16,17] and Rouxel et al.[18] by treating $Na_x(H_2O)_yTiS_2$ ($x \approx 0.5$) in 1 M aqueous solutions containing alkaline earth salts or using calcium metal in liquid ammonia, respectively. Electrochemical intercalation was recently reported using $Ca(BF_4)_2$ dissolved in a mixture of alkyl carbonate solvents as electrolyte,[13] which enables successful calcium plating and stripping at 100 °C.[7] While the reversibility of the redox process was clearly ascertained, reduction of TiS_2 proceeded through the formation of diverse phases, some of them involving a cation-solvated intercalation mechanism and hence leading to a substantial expansion of the lattice along the *c* axis. Thus, further research was undertaken using alternative electrolyte salts, such as $Ca(TFSI)_2$ (Calcium Bis(trifluoromethanesulfonimide), as the highly delocalized charge in the anions diminish tendency to ion pair formation,[19] as showed by Armand and co-workers for LiTFSI.[20] The absence of contact ion pair with TFSI-based electrolyte results in lower desolvation energy[19] at the electrolyte/electrode interface and thus potentially has an impact on the overall kinetics of calcium insertion. However, the absence of calcium plating/striping in such electrolyte[7] prevented assembly of a full cell using calcium metal anodes, and hence activated carbon (AC) was used instead as counter electrode (CE).[12]

Experimental

Electrodes were prepared using commercial TiS_2 from Aldrich (purity 99.995%) as active material mixed with carbon black (Super P, Timcal, Switzerland) and polyvinylidene difluoride (Arkema) in weight ratios of 80:10:10. A slurry was made by dispersing the active material, carbon and binder powders in N-methyl-2-pyrrolidone (Aldrich, ⩾99.9%), which was then ball milled at 400 rpm for 1 h in planetary ball miller, doctor blade casted on 18 μm thick aluminum foil (Goodfellow, 99%) and vacuum dried at 120 °C for 3 h. Since TFSI anions are known to cause corrosion of aluminium in liquid electrolytes,[21,22] electrodes were also casted on 25 μm thick stainless steel foil (Goodfellow, 99.99%). The tape, doctor blade casted with a thickness of 400 μm, was cut into discs of 11 mm diameter and pressed at 8 Tons before use, with a final loading of about 1.3 mg cm^{-2}.[23] Electrochemical tests were performed in three-electrode Swagelok cells using Ca metal (AlfaAesar, 99.5%) or AC (Kynol, ACC-509220) as counter electrodes (CE). Either Ca metal or an Ag wire were used as reference electrodes (RE). The electrolytes used were 0.3 M $Ca(BF_4)_2$ dissolved in a 1:1 mixture of ethylene carbonate (EC, Aldrich anhydrous 99.0%) and propylene carbonate (PC, Aldrich anhydrous 99.0%), prepared from $Ca(BF_4)_2 \cdot x\ H_2O$ salt (Alfa Aesar), or 0.3 M $Ca(TFSI)_2$ (Solvionic, 99.5%) in PC (Aldrich anhydrous 99.7%). The water content in all the electrolytes was measured by Karl Fisher titration and found to be lower than 50 ppm. Electrolyte preparation and cell assembling were

*Electrochemical Society Member.
[z]E-mail: rosa.palacin@icmab.es

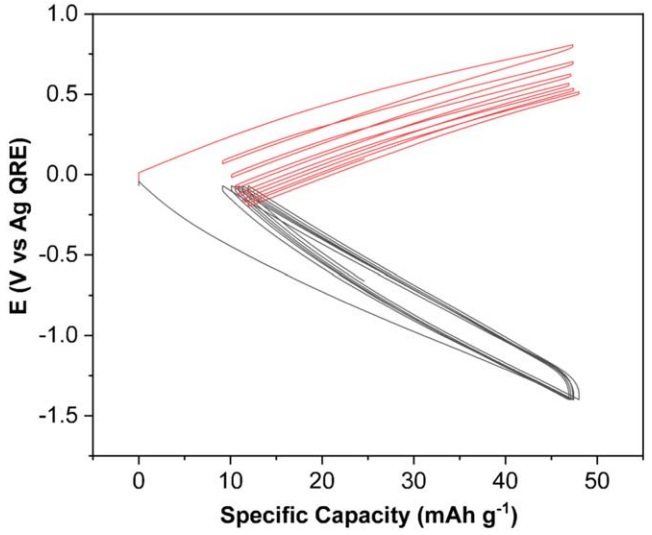

Figure 1. Capacity vs potential measured vs the Ag QRE for both AC electrodes in a symmetric cell. In such cell configuration charge is being stored by adsorption of cations on the negative electrode (black curve) and anions on the positive electrode (red curve).

done in Ar filled glove box with less than 1 ppm of O_2 and H_2O. Prior to cycling, equilibration of the working electrode (WE) under the operating conditions at open circuit potential (OCP) was ensured. Cells were cycled using a Bio-Logic VMP3 potentiostat in galvanostatic mode with potential limitation (GCPL) at C/50 and C/100 and various temperatures from room temperature to 100 °C. The stability at OCP of the as prepared TiS_2 electrodes under our experimental conditions was ascertained by immersion in the corresponding electrolytes inside two-electrode Swagelok cells for 30 to 100 h at the test temperatures followed by XRD. Twin cells were systematically assembled to assess reproducibility of results. The Ag wire quasi-reference electrode (QRE) was calibrated using a 10 mM ferrocene solution in a 0.3 M $Ca(TFSI)_2$, EC:PC electrolyte solution. The cyclic voltammetry was performed at 20 mV s^{-1} between 1.2 V and −1 V in a Swagelok three electrode configuration using stainless steel 316L as working electrode, 10 mg of carbon cloth as CE and the Ag wire as QRE.

X-Ray powder diffraction patterns were acquired in a Bruker D8 Advance A25 diffractometer in a Debye–Scherrer configuration equipped with Mo Kα1 radiation source (λ = 0.7093 Å) and Johansson monochromator. The samples, either pristine TiS_2, or powder recovered from stability tests or cycled electrodes after dismantling the electrochemical cells inside Ar filled glove box, were embedded in a 0.5 mm diameter borosilicate glass capillary, and rotated during data collection.

Results and Discussion

Assessment of electrochemical set up.—In conventional battery technologies, such as Li-ion, the reliability of conventional experimental protocols is well established. Yet, the know how gained can seldom be translated to alternative chemistries and the establishment of standards (such as RE or electrolyte) is far from being trivial.[12] Moreover, in absence of rigorous methodologies experiments can lead to misleading conclusions due to existence of side reactions (e.g. corrosion of current collector).[24] Thus, the first part of this work involved the reliability assessment for the experimental setup to be used. Since the aim was to explore reactivity under different conditions, the study involved the use of different electrolytes, which, in turn, forced to diverse options for CE and current collector.

Indeed, following on our previous work,[13] the first option was to use $Ca(BF_4)_2$ dissolved in a mixture of EC and PC as electrolyte, since this formulation enables reversible calcium plating and stripping at high temperature, and hence Ca metal CE can be used. Moreover, no corrosion of Al takes place, which makes possible to use this metal as current collector. This approach does also involve some drawbacks, as commercial $Ca(BF_4)_2$ is typically hydrated,[25,26] and hence drying is compulsory to avoid water molecules being present in the electrolyte, which would in turn induce parasitic redox reactions and partial hydrolysis of BF_4^- to yield HF. Moreover, the drying protocol is somewhat problematic, as hydrolysis in the crystallization water can be thermally induced. In contrast, anhydrous $Ca(TFSI)_2$ based electrolytes are easy to achieve and despite not enabling plating/stripping, exhibit higher ionic conductivity and lower degree of contact ion pair for a given salt concentration when compared to $Ca(BF_4)_2$ based ones.[19] Thus, electrochemical tests were also performed using $Ca(TFSI)_2$ in PC as alternative, which forced the use of a different CE alternative to Ca metal, but at the same time enabled screening a wider range of conditions, including room temperature. Activated carbon (AC) was used for that purpose, which operates not through a faradaic but through a capacitive mechanism, with charge being stored electrostatically through ions adsorption on the carbon's wide specific surface area (no charge transfer involved). The advantages of using AC include high reversibility, operation window matching the stability of most electrolytes and versatility in terms of ions that can be adsorbed. Yet, its relatively low specific capacity requires careful cell balancing to make sure the CE is significantly oversized with respect to the expected capacity of the WE. In Fig. 1, GCPL curves of such AC electrode in 0.3 M $Ca(TFSI)_2$ in EC:PC (room temperature) is shown. As expected, pure capacitive GCPL profile is observed with a constant variation of the potential with the capacity and a specific capacity of about 35 mAh.g^{-1} recorded for AC electrodes at 25 mA.g^{-1}, within 0 and −1.4 V vs Ag QRE (see Fig. 1).

All tests presented in the following sections were performed ensuring an oversizing of the AC CE capacity when compared to the TiS_2 WE by at least a factor of 3.7. Because the potential of the carbon electrode varies with the capacity, three electrode cells were assembled using Ag wire QRE, which was calibrated using a ferrocene/ferrocenium solution as described in the experimental section, its potential being 0.381 V vs NHE.

The use of 316 stainless steel current collectors was also compulsory as they present higher corrosion resistance in TFSI-based electrolyte, with an onset potential for corrosion about 600 mV higher than when Al is used.[12] Thus, compatibility with TiS_2 electrode operation potential is expected despite the possibility of some corrosion upon oxidation not being fully excluded.

Electrochemical reactivity of TiS_2.—In line with the aspects discussed in the previous section, assessing electroactivity of potential electrode materials in new battery chemistries can be problematic. Even using a proper experimental setup and with the observation of a redox process, activity of the material cannot be taken for granted. Indeed, side reactions may occur and the use of complementary characterization techniques is compulsory to assess electrode reactivity. Thus, and in order to get further insights on the reactivity of TiS_2 in calcium electrolytes, a series of experiments was carried out, consisting on a single reduction followed by XRD. These were carried out using $Ca(BF_4)_2$ in EC:PC or $Ca(TFSI)_2$ in PC electrolytes, at three different temperatures: room temperature, 60 °C and 100 °C and two rates C/50 and C/100, with a very low potential cut off (−4 V), to ensure that if intercalation was feasible it would be observed, even if cell polarization was high. Since experiments involved a single reduction of the working electrode and hence stripping at the counterelectrode, Ca metal anodes were used in all cases for the sake of simplicity. Figure 2a displays the characteristic voltage vs capacity profiles of TiS_2 electrodes subjected to GCPL tests at 100 °C and C/100 rate in three-electrode cells using Ca metal CE and 0.3 M $Ca(BF_4)_2$, EC:PC and $Ca(TFSI)_2$, PC electrolytes. The corresponding ex situ XRD patterns, collected after full reduction, are shown in Fig. 2b.

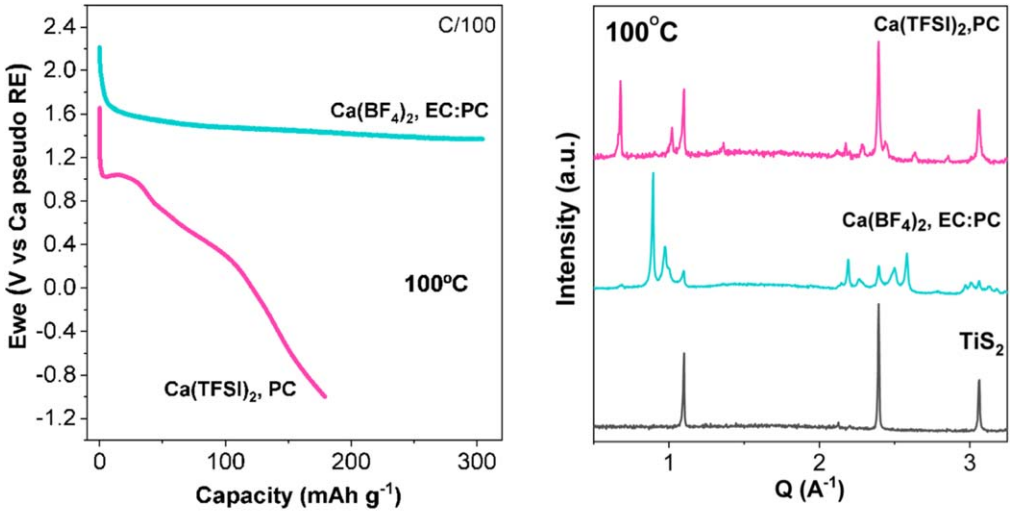

Figure 2. GCPL voltage vs capacity profiles at 100 °C and C/100 rate of Ca//TiS_2 cells, in $Ca(BF_4)_2$, EC:PC(pink curve) and $Ca(TFSI)_2$, PC(blue curve) electrolytes (a) and corresponding ex situ XRD diffractograms (b). The characteristic XRD pattern of TiS_2 pristine electrode is also displayed for comparison.

As can be deduced from Fig. 2a, the potential vs capacity profile of TiS_2 is strongly dependent on the electrolyte used: it evolves through a pseudoplateau centred at about 1.6 V (vs Ca pseudo reference electrode) in $Ca(BF_4)_2$, EC:PC and through a multi-step, sloping trend with some discontinuities at about 1 V and 0.2 V (vs Ca pseudo REF) in $Ca(TFSI)_2$, PC electrolyte. Specific capacities approach 300 and 185 mAh g^{-1} respectively, which would correspond to about 0.6 and 0.4 mol of inserted Ca^{2+} ions per mol of TiS_2 if this was the only redox process taking place. Yet, contributions to the observed values of capacity from electrolyte decomposition side reactions must be reasonably taken into account, especially considering the high temperature and very low rate employed for the electrochemical tests. The ex situ XRD patterns corresponding to the samples recovered after this first reduction are displayed in Fig. 2b and indicate that despite some TiS_2 remains unreacted, additional phases are formed, which are different depending on the electrolyte. Some minor peaks corresponding to CaF_2 most likely formed from electrolyte decomposition reactions, are observed at Q values of 2.19 and 2.15 $Å^{-1}$. In addition to those, extra reflections appear at Q values of 0.89, 0.97, 2.58, 2.5 and 2.26 $Å^{-1}$ for the $Ca(BF_4)_2$ case and at 0.68, 1.02, 2.28 and 2.44 $Å^{-1}$ for $Ca(TFSI)_2$. According to our previous study, [13] these peaks can be reasonably ascribed to i) a solvent co-intercalated phase with largely expanded c parameter (main reflection at 0.68 $Å^{-1}$), ii) Ca_xTiS_2 phase with $x \sim 0.5$, already reported by J. Rouxel et al.,[18] peaks at 0.89 and 2.58 $Å^{-1}$ and iii) a second stage-type intercalate (main peaks around 1, 2.2 and 2.5 $Å^{-1}$), each phase being formed at the expense of pristine TiS_2. While the same type of products is formed in both electrolytes upon reduction, the relative amounts of each phase are very strongly dependent on the electrolyte used. Indeed, and in contrast with what is observed for $Ca(BF_4)_2$, Ca_xTiS_2 is never formed for $Ca(TFSI)_2$ in PC electrolyte, even if reduction is pursued to lower potentials (tests not shown here). GCPL tests were also carried out at 60 °C and room temperature in three-electrode cells using AC CE (since cycling tests were performed), in both electrolytes. In the case of $Ca(BF_4)_2$ ex situ XRD do only indicate the presence of unreacted TiS_2 (data not shown here) while for $Ca(TFSI)_2$ patterns were similar to those achieved at 100 °C with Ca CE, both at C/100 and C/50 rates (see Fig. 3). XRD patterns collected at different stages of reduction reveal the progressive growth of relative intensity of the inserted phases at the expense of pristine TiS_2. The potential vs capacity profile exhibits sloping voltage, with discontinuities at about −0.8 and −2.2 V (vs Ag QRE) with capacities of about 150–200 mAh g^{-1} at C/100 between 0 to −5 V vs Ag QRE. XRD patterns are very similar to those achieved when the experiments are carried out at 100 °C. In view of such results, we undertook cycling tests at both room temperature and 60 °C using 0.3 M $Ca(TFSI)_2$ in PC as electrolyte and AC CE. The representative galvanostatic cycling voltage vs capacity profiles at C/100 rate of the cell cycled at RT is displayed in Fig. 3a, together with the corresponding ex situ XRD patterns at the end of reduction and after complete reoxidation.

A specific capacity of about 140 mAh g^{-1} is achieved at RT and a significant voltage hysteresis is observed (see Fig. 3a). The oxidation steps need to be capacity limited, as they would evolve through a continuous plateau, that, besides calcium de-intercalation, may reasonably be related to corrosion of stainless steel current collector/electrolyte side reactions that need further investigation. In order to ensure that full oxidation was achieved even in presence of side reactions, the cells were overcharged. The ex situ XRD patterns of the TiS_2 after full reduction and oxidation at room temperature (plots A and B) are depicted in Fig. 3b and confirm the complete reversibility of the calcium intercalation process, as TiS_2 is the only phase present in re-oxidized electrodes, despite with somewhat broader peaks, which may be related to strain/defects. Analogous results were obtained after multiple cycles at 60 °C (data not shown). Since no contact ion pairs are formed in 0.3 M $Ca(TFSI)_2$-PC electrolyte, the Ca^{2+} are solely solvated by PC. Although it is not clear how many solvent molecules are being co-intercalated with Ca^{2+}, one can speculate that 1 to 2 PC molecules maximum could be co-intercalated in the available interlayer space. The fact that the insertion process was found to be fully reversible demonstrates PC molecules are deintercalated together with Ca^{2+} upon oxidation and no solvent trapping takes place.

Figure 4a depicts the patterns collected at various redox stages for cells tested at 60 °C and confirm the reversibility of the process. LeBail fitting carried out using Fullprof program was carried out for the XRD patterns corresponding TiS_2 electrodes recovered from cells tested in $Ca(TSFI)_2$ PC at RT (full reduction) and 60 °C (half and full reduction). The profile fit for the latter is shown in Fig. 4b as an example, and the cell parameters for the phases present and agreement factors are depicted in Table I. The cell parameters obtained for the TiS_2 phase are the same as those achieved for the pristine sample in all cases, in agreement with no solid solution formation. The additional diffraction peaks present in the patterns are consistent with two of the three hexagonal phases with an expanded c parameter which were previously observed in $Ca(BF4)_2$ electrolytes.[13] These were denoted as phase 1 and phase 3, with the

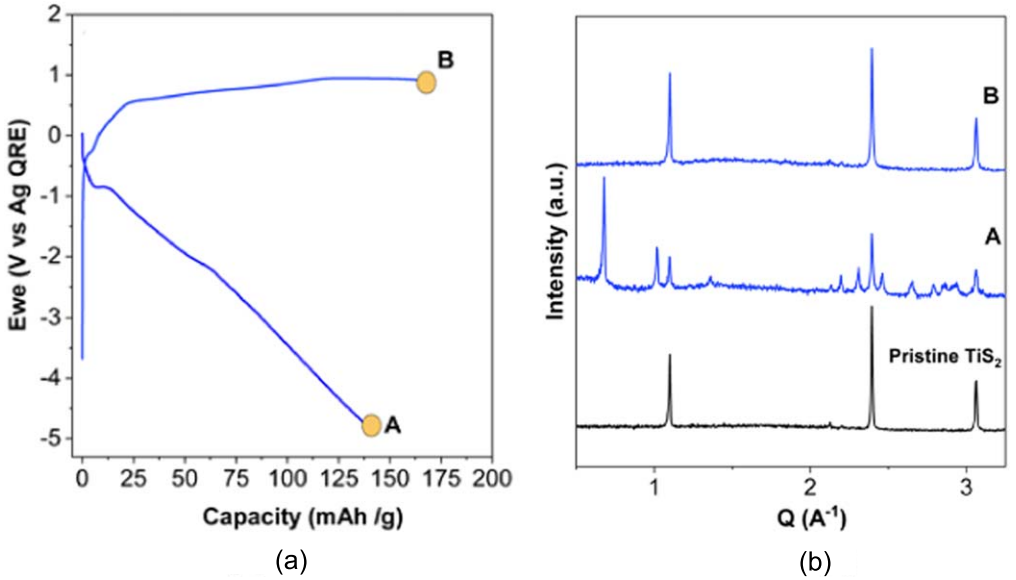

Figure 3. GCPL voltage vs capacity profiles of AC//TiS_2 cells using $Ca(TFSI)_2$ in PC as electrolyte at RT C/100 rate, (a) and corresponding ex situ XRD patterns (b). The pattern corresponding to pristine TiS_2 is also represented.

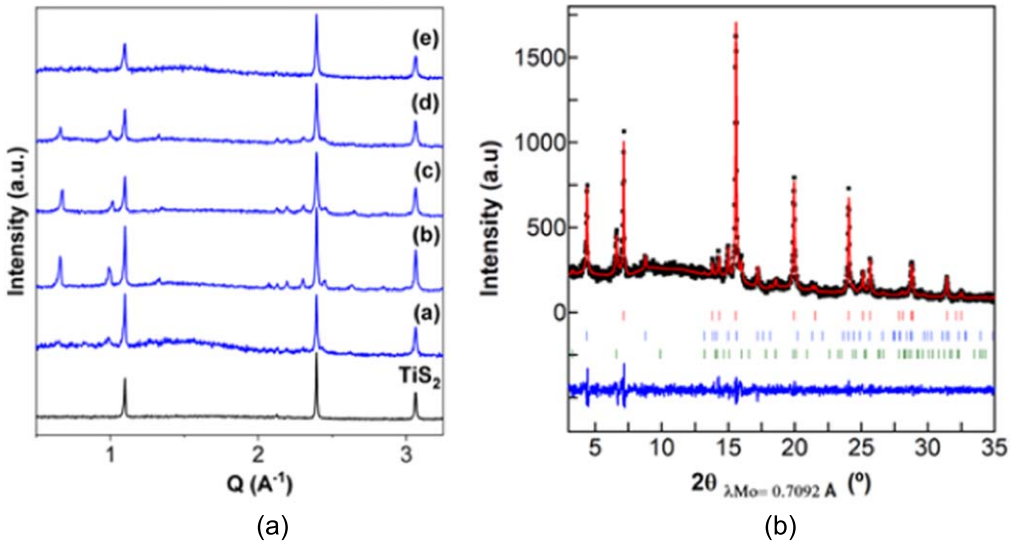

Figure 4. XRD patterns corresponding to pristine TiS_2 and samples recovered from cells at early stage of reduction (−0.75 V) (a), half-reduction (−2.5 V) (b), end of reduction (−4 V) (c), half-oxidation (0.4 V) (d) and full oxidation (e) in AC/$Ca(TFSI)_2$, PC/TiS_2 cells tested at 60 °C at C/100. (a) Le Bail profile fitting corresponding to pattern (c), upper ticks correspond to calculated reflections of TiS_2 (red) and middle and lower ticks to calculated reflections for co-intercalated and stage2 type phases in the hexagonal system space group R-3m, blue and green respectively. (b).

Table I. Cell parameters and agreement factors obtained for the Le Bail profile fitting of the ex situ XRD patterns corresponding to TiS_2 electrodes after reduction in $Ca(TSFI)_2$ PC at RT under different conditions.

		$Ca(TSFI)_2$, PC at RT (−4.7 V)	$Ca(TSFI)_2$, PC at 60°C (−2.5 V)	$Ca(TSFI)_2$, PC at 60°C (−4 V)
TiS_2 *(P-3m1)*	a (Å)	3.4018(2)	3.40376(13)	3.4023(2)
	c (Å)	5.6941(7)	5.6941(4)	5.6928(5)
	V ($Å^3$)	57.07(1)	57.08(1)	57.07(1)
Phase 1 *(R-3m)*	a (Å)	3.4070(4)	3.40914(27)	3.4089(3)
	c (Å)	27.75(6)	28.321(5)	27.757(4)
	V ($Å^3$)	278.94(8)	284.81(6)	279.35(6)
Phase 3 *(R-3m)*	a (Å)	3.3535(4)	3.3578(6)	3.3595(6)
	c (Å)	36.986(4)	37.730(6)	36.921(6)
	V ($Å^3$)	360.22(7)	367.1(2)	360.9(1)
	R_p	7.6	7.91	6.55
	χ^2	1.77	1.61	1.43

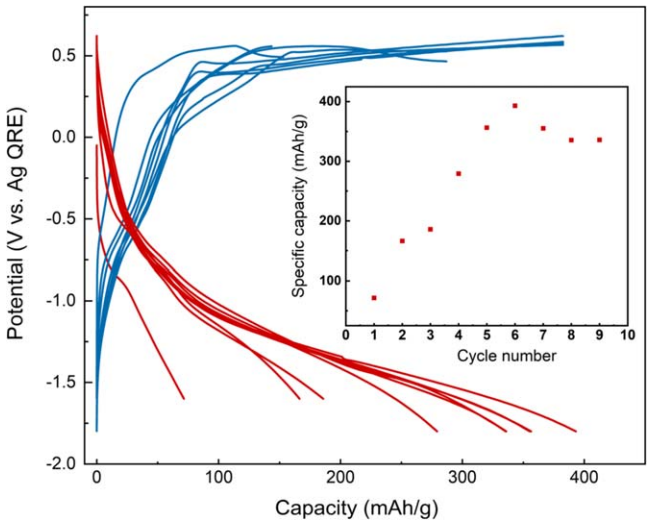

Figure 5. Electrochemical curves corresponding to a TiS_2 cell with activated carbon as counter electrode, an Ag wire reference and 0.3 M $Ca(TFSI)_2$ in PC as electrolyte tested at C/50 rate and at 60 °C. Inset depicts specific capacity achieved upon reduction as a function of cycle number.

cell parameters being consistent with a solvent co-intercalated phase and a second stage-type intercalate respectively. Their cell parameters of seem to exhibit small deviations at different redox stages in agreement with different content of intercalated species.

Figure 5 shows the voltage vs capacity profiles for AC// TiS_2 three-electrode cells upon further cycling at 60°C and C/50. A significant increase in capacity is observed after the first cycle, together with some reduction in the hysteresis. One could speculate that minor structural changes (e.g. creation of defects) taking place upon the first redox cycle might facilitate larger insertion degrees in the following cycles. Yet, the existence of side reactions related to the electrolyte and/or the current collector cannot be ruled out. A study of the redox mechanism and the relative evolution of the two phases formed at different degrees of oxidation/reduction via operando diffraction should also give some insight in these aspects.

Conclusions

Overall, these results indicate that reversible electrochemical insertion of calcium in TiS_2 takes place in $Ca(TFSI)_2$ in PC as electrolyte at 100 °C, 60 °C and even room temperature via the formation of solvent co-intercalated phases. While still being far from practical prospects or theoretical figures of merit,[1] these results open some positive prospects in the achievement of proof-of-concept for calcium batteries. Nonetheless, diverse crucial aspects remain to be fully understood such as the dependence of phases formed on the electrolyte structure and solvation energies. Recent development in new electrolytes enabling reversible calcium metal stripping/deposition at room temperature,[9,10] together with the awareness that mastering the Ca metal interphase will hopefully contribute to improve practical performance.

Finally, the experimental results achieved contribute to the establishment of reliable and viable cell set-up and methodology for the unambiguous study of the intercalation process in multivalent battery systems, for which the protocols given for granted in lithium ion batteries do not hold anymore.

Acknowledgments

Funding from the European Union's Horizon 2020 research and innovation programme H2020 FETOPEN-1-2016-2017 (CARBAT, grant agreement No. 766617) and ERC-2016-STG, (CAMBAT grant agreement No 715087) is gratefully acknowledged. Authors are grateful to the Spanish Ministry for Economy, Industry and Competitiveness Severo Ochoa Programme for Centres of Excellence in R&D (SEV-2015-0496).

ORCID

A. Ponrouch https://orcid.org/0000-0002-8232-6324
M. R. Palacin https://orcid.org/0000-0001-7351-2005

References

1. D. Monti, A. Ponrouch, R. B. Araujo, F. Barde, P. Johansson, and M. R. Palacin, *Front. Chem.*, **7**, 79 (2019).
2. J. Muldoon, C. B. Bucur, and T. Gregory, *Chem. Rev.*, **114**, 11683 (2014).
3. P. Canepa, G. S. Gautam, D. C. Hannah, R. Malik, M. Liu, K. G. Gallagher, K. A. Persson, and G. Ceder., *Chem. Rev.*, **117**, 4287 (2017).
4. M. E. Arroyo-de Dompablo, A. Ponrouch, P. Johansson, and M. R. Palacin, *Chem. Rev.*, (2019).
5. D. Aurbach, X. Lu, A. Schechter, Y. Gofer, H. Gizbar, R. Turgeman, Y. Cohen, M. Moshkovich, and E. Levi, *Nature*, **407**, 724 (2000).
6. X. Sun, P. Bonnick, V. Duffort, M. Liu, Z. Rong, K. A. Persson, G. Ceder, and L. Nazar., *Energy Environ. Sci.*, **9**, 2273 (2016).
7. A. Ponrouch, C. Frontera, F. Barde, and M. R. Palacin, *Nat. Mater.*, **15**, 169 (2016).
8. D. Wang, X. Gao, Y. Chen, L. Jin, C. Kuss, and P. G. Bruce, "Plating and stripping calcium in an organic electrolyte." *Nat. Mater.*, **17**, 16 (2018).
9. Z. Li, O. Fuhr, M. Fichtner, and Z. Zhao-Karger, *Energy Environ. Sci.*, **12**, 3496 (2019).
10. A. Shyamsunder, L. E. Blanc, A. Assoud, and L. F. Nazar, *ACS Energy Lett.*, **4**, 2271 (2019).
11. D. S. Tchitchekova, D. Monti, P. Johansson, F. Barde, A. Randon-Vitanova, M. R. Palacin, and A. Ponrouch, *J. Electrochem. Soc.*, **164**, A1384 (2017).
12. R. Dugas., J. D. Forero-Saboya, and A. Ponrouch, *Chem. Mat.*, **31**, 8613 (2019).
13. D. S. Tchitchekova, A. Ponrouch, R. Verrelli, T. Broux, C. Frontera, A. Sorrentino, F. Barde, N. Biskup, E. Arroyo-de Dompablo, and M. R. Palacin, *Chem. Mater.*, **30**, 847 (2018).
14. M. S. Whittingham, *Prog. Solid State Chem.*, **12**, 41 (1978).
15. M. Gauthier et al., *J. Electrochem. Soc.*, **132**, 1333 (1985).
16. R. Schöllhorn and H. Meyer, *Mat. Res. Bull.*, **9**, 1237 (1974).
17. A. Lerf and R. Schöllhorn, *Inorg. Chem.*, **16**, 2950 (1977).
18. A. Le Blanc-Soreau and J. Rouxel, *C.R. Acad. Sc. Paris*, **279**, C303 (1974).
19. J. D. Forero-Saboya, E. Marchante, R. B. Araujo, D. Monti, P. Johansson, and A. Ponrouch, *J. Phys. Chem. C*, **123**, 29524 (2019).
20. S. Atchia, W. Gorecki, M. Armand, and D. Deroo, *Electrochim. Acta*, **37**, 1743 (1992).
21. B. Garcia and M. Armand, *J. Power Sources*, **132**, 206 (2004).
22. M. Morita, T. Shibata, N. Yoshimoto, and M. Ishikawa, *Electrochim. Acta*, **47**, 2787 (2002).
23. A. Ponrouch and M. R. Palacin, *J. Power Sources*, **196**, 9682 (2011).
24. A. L. Lipson, D. L. Proffit, B. Pan, T. T. Fister, C. Liao, A. K. Burrell, J. T. Vaughey, and B. J. Ingram, *J. Electrochem. Soc.*, **162**, A1574 (2015).
25. R. de Pape, J. Ravez, and P. Pascal, *Comptes Rendus de l'Academie des Sciences*, **254**, 4171 (1963).
26. J. L. Leibenguth, *Bull. Soc. Chim. France*, **12**, 3811 (1966).